# The ER stress sensor inositol-requiring enzyme 1α in Kupffer cells promotes hepatic ischemia-reperfusion injury

Jie Cai[1], Xiaoge Zhang[1], Peng Chen[1], Yang Li[1], Songzi Liu[1], Qian Liu[1], Hanyong Zhang[2], Zhuyin Wu[1], Ke Song[2], Jianmiao Liu[3], Bo Shan[4,*], and Yong Liu[1,*]

From the [1]Hubei Key Laboratory of Cell Homeostasis, College of Life Sciences, the Institute for Advanced Studies, Frontier Science Center for Immunology and Metabolism, Wuhan University, Wuhan, China; [2]Department of Stomatology, Tongji Hospital, Tongji Medical College, and [3]Cellular Signaling Laboratory, Key Laboratory of Molecular Biophysics of Ministry of Education, Huazhong University of Science and Technology, Wuhan, China; [4]Touchstone Diabetes Center, Department of Internal Medicine, University of Texas Southwestern Medical Center, Dallas, Texas, USA

Edited by Ursula Jakob

Hepatic ischemia/reperfusion (I/R) injury is an inflammation-mediated process arising from ischemia/reperfusion-elicited stress in multiple cell types, causing liver damage during surgical procedures and often resulting in liver failure. Endoplasmic reticulum (ER) stress triggers the activation of the unfolded protein response (UPR) and is implicated in tissue injuries, including hepatic I/R injury. However, the cellular mechanism that links the UPR signaling to local inflammatory responses during hepatic I/R injury remains largely obscure. Here, we report that IRE1α, a critical ER-resident transmembrane signal transducer of the UPR, plays an important role in promoting Kupffer-cell-mediated liver inflammation and hepatic I/R injury. Utilizing a mouse model in which IRE1α is specifically ablated in myeloid cells, we found that abrogation of IRE1α markedly attenuated necrosis and cell death in the liver, accompanied by reduced neutrophil infiltration and liver inflammation following hepatic I/R injury. Mechanistic investigations in mice as well as in primary Kupffer cells revealed that loss of IRE1α in Kupffer cells not only blunted the activation of the NLRP3 inflammasome and IL-1β production, but also suppressed the expression of the inducible nitric oxide synthase (iNos) and proinflammatory cytokines. Moreover, pharmacological inhibition of IRE1α's RNase activity was able to attenuate inflammasome activation and iNos expression in Kupffer cells, leading to alleviation of hepatic I/R injury. Collectively, these results demonstrate that Kupffer cell IRE1α mediates local inflammatory damage during hepatic I/R injury. Our findings suggest that IRE1α RNase activity may serve as a promising target for therapeutic treatment of ischemia/reperfusion-associated liver inflammation and dysfunction.

Hepatic ischemia/reperfusion (I/R) injury represents one of the major complications occurring during liver resection, transplantation, hypovolemic shock, and other liver surgeries, which causes increased risk of organ rejection and liver dysfunction (1–3). Hepatic I/R injury is viewed as a dynamic two-phase process that involves local ischemic stress and inflammation-mediated reperfusion damage in the liver (1, 2, 4–6). Hepatic I/R injury is initiated by the ischemic insult that leads to cellular damage and cell death of hepatocytes *via* oxidative stress and reactive oxygen species (ROS) production, triggering a local sterile immune response characterized by recruitment of Kupffer cells (KCs) and neutrophils. Propagation of the innate and adaptive immune responses in turn results in elevated cytokine production, further aggravating hepatocyte cell death and necrotic damage in the liver (1, 6, 7). Many intracellular signaling cascades in multiple cell types in the liver, including hepatocytes and immune cells as well, have been implicated in the mechanisms underlying the inflammation-mediated injury as a result of the ischemia/reperfusion-elicited stress (1–6, 8, 9). For instance, emerging evidence indicates that KCs, the liver-resident specialized macrophages (10, 11), play crucial roles in orchestrating the initial innate immune responses through phagocytosing necrotic cells, producing proinflammatory cytokines, and recruiting other inflammatory cells including neutrophils and circulating monocytes, thus driving local inflammation in the liver upon I/R injury (4–7, 12). Moreover, it has been documented that the nucleotide-binding domain, leucine-rich repeat containing protein 3 (NLRP3) critically contributes to the sterile inflammatory response and liver damage during hepatic I/R injury, either through activation of inflammasome in KCs (4–6) or *via* affecting the recruitment of neutrophils (6, 13). In addition, inducible nitric oxide synthase (iNos), a cytokine-regulated enzyme that converts L-Arginine to L-Citrulline and nitric oxide (NO) in many types of cells including immune cells such as macrophages (14–17), has been documented to be involved in inflammation-mediated tissue injury, while its exact roles in hepatic I/R injury have been controversial (18–20). Importantly, hepatic I/R injury remains to be a clinically unsolved problem lacking effective intervention strategies. Therefore, it is of particular translational significance to improve our understanding of the

cellular immune events that mediate local inflammatory responses and ultimately cause I/R-induced liver injury and dysfunction.

Endoplasmic reticulum (ER) stress is instigated by increased accumulation of unfolded/misfolded proteins in the ER lumen (21, 22). ER stress activates the cellular unfolded protein response (UPR) regulated by three ER-resident transmembrane signal transducers, inositol-requiring enzyme 1 (IRE1), protein kinase RNA-like endoplasmic reticulum kinase (PERK), and activating transcription factor 6 (ATF6) (22, 23). IRE1 is the most evolutionarily conserved ER stress sensor that contains the Ser/Thr protein kinase and endoribonuclease (RNase) activities within its cytoplasmic portion (24–26). Upon ER stress, IRE1 is activated through autophosphorylation and dimerization/oligomerization and catalyzes the unconventional splicing of the mRNA encoding the transcription factor X-box binding protein 1 (XBP1) or degrades selected mRNA species in a process referred to as "regulated IRE1-dependent decay" (RIDD) (24–28). ER stress has been implicated in various pathological conditions, including obesity, type 2 diabetes, cancer, as well as liver diseases (29–33). Reported studies have also revealed that the ER stress response is activated during hepatic I/R injury (34–37), with distinct biphasic activation of the UPR branches found at the two stages of hepatic I/R injury (34). It is also notable that in mouse models, IRE1α appeared to be involved in exerting a protective action from ER stress preconditioning or an aggravating effect from high-fat diet–induced fatty liver upon hepatic I/R injury (38, 39). However, the precise cellular mechanisms that link individual UPR branches to inflammatory liver damage remain largely obscure.

The IRE1α branch plays a critical role in regulating macrophage activation and inflammatory cytokine production under a variety of stress conditions (24–26, 40–43). Given its involvement in regulating macrophage inflammasome activation as well as its polarized activation states during metabolic inflammation (24–26, 44–48), we wondered if IRE1α also acts to regulate the immune responses of KCs during hepatic I/R injury. In this study, we utilized the mouse model in which IRE1α is specifically ablated in myeloid cells and investigated whether IRE1α in KCs contributes to inflammatory liver damage. We found that IRE1α in KCs mediates inflammasome activation and drives iNos expression, thus promoting hepatic I/R injury in a manner that depends on its RNase activity.

## Results

### Activation of the IRE1α pathway and NLRP3 inflammasome in Kupffer cells during hepatic I/R injury

To investigate whether the UPR signaling branch is implicated in KC activation in response to hepatic I/R injury, we established the hepatic I/R injury model in mice that were subjected to 60 min of partial warm ischemia followed by 6 h of reperfusion in the liver. Immunoblot analyses revealed elevations in IRE1α phosphorylation as well as in the spliced form of XBP1 (XBP1s) protein level, but no apparent changes

in eIF2α phosphorylation in I/R-injured livers relative to their sham control (Fig. 1A). In line with previously reported studies (6, 49), we observed robust increases in NLRP3 and cleaved Caspase 1 (c-Casp1) proteins in I/R-injured livers (Fig. 1A). This indicates marked activation of NLRP3 inflammasome, a multiprotein platform that is assembled to activate Caspase 1 for the maturation and release of the proinflammatory cytokine IL-1β (50–52). Next, we examined the UPR and inflammasome activation in KCs and hepatocytes that were freshly isolated from the livers of mice following I/R injury or sham control. Whereas more prominently increased IRE1α phosphorylation was detected in KCs than in hepatocytes from the livers after I/R injury, higher expression levels of XBP1s protein were seen in both cell types (Fig. 1B). Consistently, no increases in eIF2α phosphorylation were detected in KCs or hepatocytes (Fig. 1B). Remarkably, marked elevations in NLRP3 and c-Casp1 proteins were observed in KCs but not in hepatocytes from I/R-injured livers (Fig. 1B). Moreover, quantitative RT-PCR profiling analyses showed significantly higher levels of *Xbp1s* mRNA along with its transcriptional target gene *Erdj4* in both KCs and hepatocytes from I/R-injured livers (Fig. 1C). In parallel, significant elevations in the expression of proinflammatory genes were detected in KCs, including *Ccl2, Il1b, Il6* as well as *Nos2*, while only *Ccl2* expression was higher in hepatocytes following I/R injury (Fig. 1D). These data suggest that the IRE1α branch of the UPR can be selectively activated, which is accompanied by NLRP3 inflammasome activation, in KCs, the main cell type mediating hepatic inflammation during I/R injury.

### Myeloid IRE1α ablation results in alleviation of I/R-induced hepatic injury and inflammation

To determine whether IRE1α activation in KCs contributes to hepatic I/R injury, we used the mouse model in which the *Ern1* gene (encoding IRE1α) is specifically abrogated in myeloid cells (MΦKO) by intercrossing the *Ern1*-flox/flox mice with the *Lysozyme2*-Cre line (42). As expected, immunoblot analysis showed that IRE1α protein expression was completely abolished in KCs but not in hepatocytes of MΦKO mice in comparison with flox/flox control animals (Fig. 2A), which led to an efficient reduction in *Xbp1s* mRNA level specifically in KCs with or without I/R injury (Fig. 2B). However, IRE1α abrogation did not result in alterations in the mRNA expression of typical UPR genes, such as *Atf4, Bip,* or *Chop,* either in KCs or in hepatocytes (Fig. S1). Relative to their control counterparts, MΦKO mice exhibited significantly less hepatic necrotic area (Fig. 2C), lower serum alanine aminotransferase (ALT) and aspartate aminotransferase (AST) levels (Fig. 2D), and decreased cell death in their livers (Fig. 2E) following hepatic I/R procedure. Moreover, immunostaining assessment showed that loss of IRE1α led to significant reductions in Ly6G^{+} neutrophil infiltration induced by hepatic I/R injury in the livers of MΦKO mice relative to their sham controls (Fig. 3A). In parallel, significantly lower serum levels of proinflammatory cytokines/chemokines were detected in
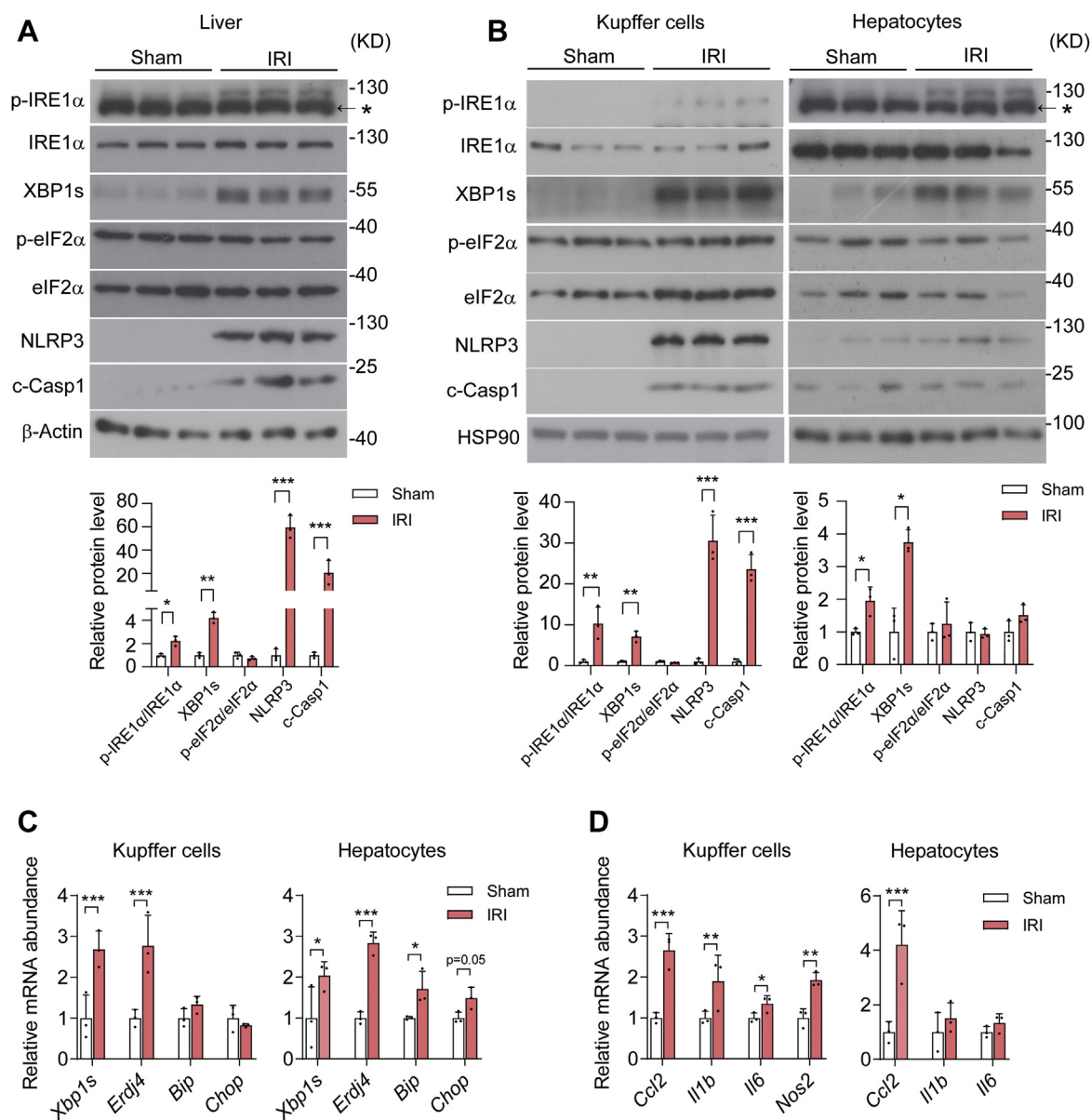
**Figure 1. The IRE1α pathway is activated in parallel with the NLRP3 inflammasome in Kupffer cells upon hepatic ischemia/reperfusion.** Male C57BL6 mice were subjected to 60 min of partial hepatic warm ischemia followed by 6 h of reperfusion to induce hepatic ischemia/reperfusion injury (IRI), and sham-treated mice were used as control (n = 3 per group). *A,* immunoblot analysis of the indicated proteins in whole liver lysates. The *asterisk* indicates the nonspecific band detected by the phospho-IRE1α antibody. β-Actin was used as the loading control. Shown also is quantification of IRE1α and eIF2α phosphorylation as well as XBP1s, NLRP3, and c-Casp1 protein levels. *B,* immunoblot analysis of the indicated proteins in cell lysates of freshly isolated Kupffer cells and hepatocytes from livers of the IRI and sham control group. The *asterisk* indicates the nonspecific band detected in hepatocytes by the phospho-IRE1α antibody. HSP90 was used as the loading control. Shown also is quantification of IRE1α and eIF2α phosphorylation as well as the indicated proteins. *C,* quantitative RT-PCR (qRT-PCR) analysis of mRNA abundance of the indicated UPR genes in freshly isolated Kupffer cells and hepatocytes. *D,* qRT-PCR analysis of mRNA abundance of the indicated inflammatory genes in freshly isolated Kupffer cells and hepatocytes. Data are shown as the mean ± SD. *$p < 0.05$, **$p < 0.01$, and ***$p < 0.001$ by unpaired two-tailed Student's *t* test. NLRP3, nucleotide-binding domain, leucine-rich repeat containing protein 3; UPR, unfolded protein response.

MΦKO animals following hepatic I/R injury, including IL-1β, CCL2, TNFα, and CXCL10 (Fig. 3B). Interestingly, significantly reduced mRNA expression levels of *Ccl2* and *Nos2* (encoding iNos protein), but not *Il1b*, were observed in KCs isolated from I/R-injured MΦKO livers (Fig. 3C), whereas no significant reduction in *Ccl2*, *Il1b* or *Nos2* expression was seen in their hepatocytes (Fig. 3D).

To further affirm that KCs, which constitute a major portion of liver-resident macrophages (53), mediated the

observed alleviating effects of IRE1α deficiency upon hepatic I/R injury in MΦKO mice, we used clodronate liposomes that can selectively deplete tissue-resident macrophages (*e.g.*, KCs) but not neutrophils through induction of apoptosis (54). Indeed, treatment with clodronate liposomes, but not the vehicle control, could efficiently deplete liver F4/80+ macrophages in mice (Fig. 4A) and resulted in significantly lower serum ALT and AST levels (Fig. 4B), less hepatic necrotic area (Fig. 4C), decreased liver cell death (Fig. 4D), and
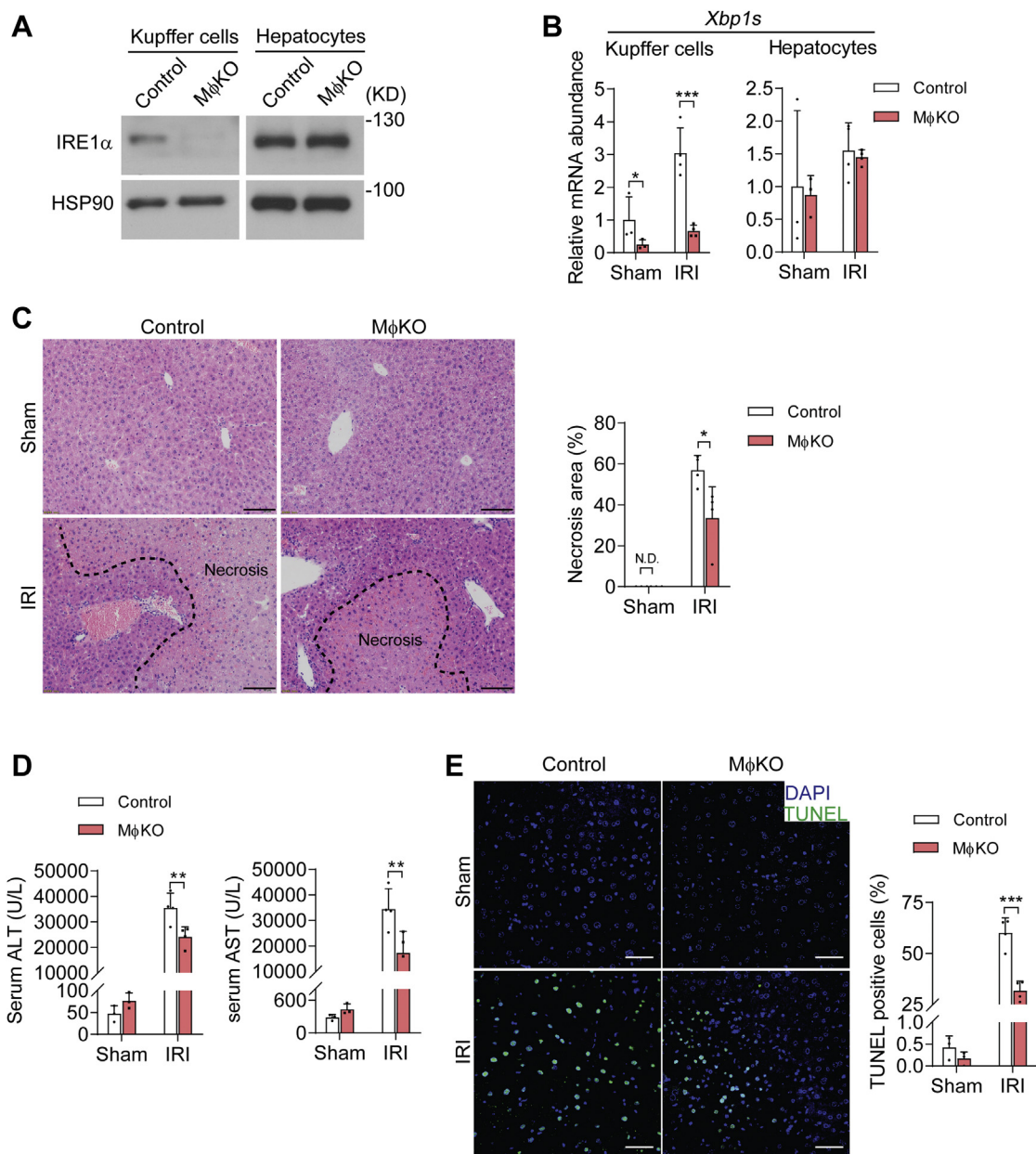
**Figure 2. Loss of myeloid IRE1α results in alleviation of hepatic I/R injury.** *A,* immunoblot analysis of IRE1α in lysates of Kupffer cells and hepatocytes freshly isolated from livers of male MΦKO mice or *Ern1*-flox/flox control littermates. HSP90 was used as the loading control. *B–E,* MΦKO or floxed control mice were subjected to sham or hepatic warm ischemia/reperfusion (n=3–4 per group). *B,* qRT-PCR analysis of mRNA abundance of *Xbp1s* in freshly isolated Kupffer cells and hepatocytes. *C,* representative images of hematoxylin and eosin staining of liver sections with the necrotic regions indicated. The area of necrosis per field was quantified (N.D., not detected). Scale bar=100 μm. *D,* serum ALT and AST levels. *E,* representative images of TUNEL staining of liver sections. TUNEL-positive cells per field were quantified. Scale bar, 15 μm. All data represent the mean ± SD. *$p < 0.05$, **$p < 0.01$, and ***$p < 0.001$ by two-way ANOVA.

reductions in Ly6G⁺ neutrophil infiltration (Fig. 4*E*) as well as serum levels of proinflammatory cytokines/chemokines (Fig. 4*F*) in control mice following hepatic I/R injury. However, we observed no further alleviating effects from clodronate treatment in I/R-injured MΦKO mice (Fig. 4, *B–F*), suggesting that the impact of IRE1α upon hepatic I/R injury was primarily mediated by its actions in liver macrophages, particularly KCs, rather than other myeloid cells such as neutrophils. Together, these results demonstrate that IRE1α deficiency in KCs protects mice against hepatic I/R injury,

indicating a role for IRE1α in KCs in mediating the inflammatory responses to promote hepatic I/R injury.

### IRE1α in Kupffer cells regulates the activation of NLRP3 inflammasome in a RNase activity-dependent manner

Next, we asked if IRE1α abrogation influenced NLRP3 inflammasome activation in KCs during hepatic I/R injury, thereby leading to lower protein production of IL-1β instead of affecting its mRNA transcription. Indeed, immunoblot
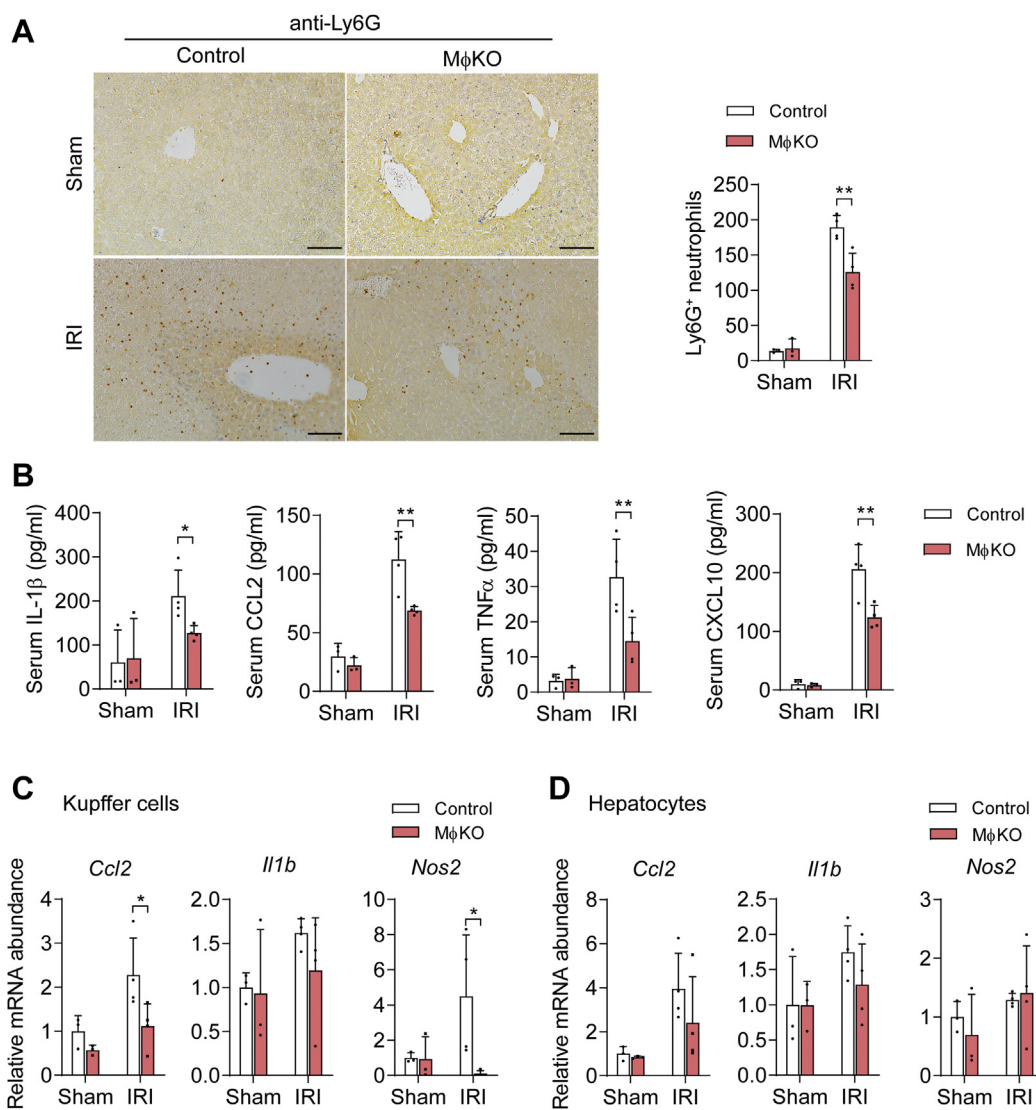
**Figure 3. Myeloid IRE1α deficiency leads to suppression of liver inflammation upon I/R injury.** MΦKO or *Ern1*-flox/flox control mice were subjected to sham or hepatic warm ischemia/reperfusion (n=3–4 per group). *A,* immunohistochemical staining of Ly6G⁺ neutrophils in liver sections of the indicated group. Quantification of Ly6G⁺ cells per field is shown. Scale bar, 100 μm. *B,* ELISA analysis of serum levels of the indicated inflammatory cytokines. *C* and *D,* qRT-PCR analysis of mRNA abundance of indicated inflammatory genes in freshly isolated Kupffer cells (*C*) or hepatocytes (*D*). All data represent the mean ± SD. **p* < 0.05 and ***p* < 0.01 by two-way ANOVA.

analyses showed significant attenuation of I/R injury-induced elevations in NLRP3 protein and Caspase 1 cleavage (c-Casp1) from MΦKO livers relative to their flox/flox control counterparts (Fig. 5*A*). Consistently, we observed that in isolated KCs but not in hepatocytes, loss of IRE1α resulted in marked reduction of XBP1s protein without affecting eIF2α phosphorylation, in parallel with lower NLRP3 protein level and more prominently reduced c-Casp1 protein level (Fig. 5*B*). To further investigate how IRE1α is involved in regulating NLRP3 inflammasome, we treated primary KCs with LPS and nigericin (NG) to fully activate NLRP3 inflammasome and IL-1β maturation (55). Whereas LPS alone could increase both XBP1s and NLRP3 protein expression levels without inducing c-Casp1 or secreted IL-1β production, LPS plus NG treatment resulted in a higher level of IRE1α phosphorylation and strongly increased c-Casp1

protein level as well as IL-1β production (Fig. 6, *A* and *B*). Interestingly, IRE1α deficiency had no significant impact upon NLRP3 protein expression but robustly blunted LPS/ NG-induced Caspase 1 cleavage and IL-1β production in MΦKO KCs (Fig. 6, *A* and *B*). Then, we used 4μ8C, a specific chemical inhibitor of IRE1α's RNase activity (56, 57), which could effectively block XBP1s protein expression (Fig. 6*C*). Remarkably, 4μ8C inhibition of IRE1α RNase resulted in significant suppression of c-Casp1 protein and secreted IL-1β production in LPS/NG-stimulated KCs without affecting NLRP3 protein expression level (Fig. 6, *C* and *D*). These data suggest that IRE1α acts through its RNase activity to promote the activation of NLRP3 inflammasome assembly in KCs, thus driving IL-1β maturation/secretion during hepatic I/R injury. Given the observed decrease of NLRP3 protein in MΦKO KCs from I/R-injured livers, it is likely that other factors or
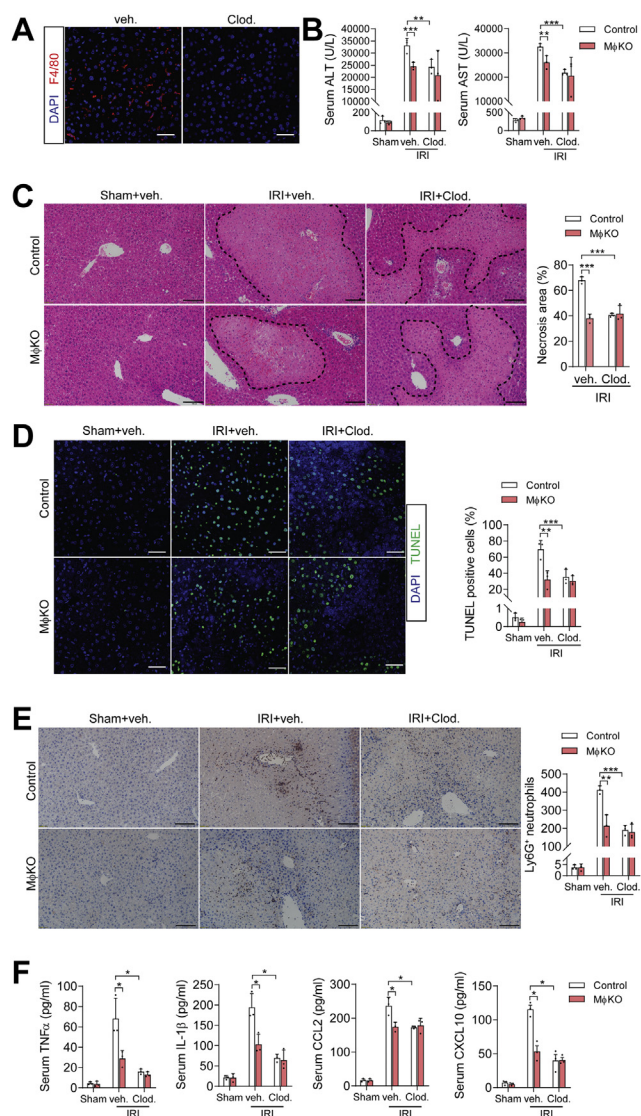
**Figure 4. Depletion of liver macrophages diminished the alleviating effects of IRE1α deficiency upon hepatic I/R injury.** MΦKO or *Ern1*-flox/flox control mice were treated through tail-vein injection with clodronate liposomes (Clod) or vehicle liposomes (200 μl per mouse). Animals were then subjected to sham or hepatic warm ischemia/reperfusion (n=3–4 per group). *A,* representative images showing clodronate depletion of F4/80[+] macrophages in liver sections of mice. Scale bar=15 μm. *B,* serum ALT and AST levels in mice of the indicated groups. *C,* representative images of hematoxylin and eosin staining of liver sections with the necrotic regions indicated. The area of necrosis per field was quantified. Scale bar=100 μm. *D,* representative images of TUNEL staining of liver sections. TUNEL-positive cells per field were quantified. Scale bar=15 μm. *E,* immunohistochemical staining of Ly6G^{+} neutrophils in liver sections. Quantification of Ly6G^{+} cells per field is shown. Scale bar=100 μm. *F,* ELISA analysis of serum levels of the indicated inflammatory cytokines. All data represent the mean ± SD. *$p < 0.05$, **$p < 0.01$, and ***$p < 0.001$ by two-way ANOVA.

additional mechanisms are involved in IRE1α regulation *in vivo* of NLRP3 inflammasome.

### IRE1α RNase in Kupffer cells promotes iNos expression during hepatic I/R injury

Because iNos is a key inflammatory mediator implicated in exacerbating liver dysfunction during I/R injury (18–20), we

investigated whether iNos expression in KCs also behaved as a downstream effector in mediating IRE1α regulation of inflammatory damage. Indeed, immunoblot analyses revealed a marked reduction in I/R injury-induced iNos protein in MΦKO livers relative to their flox/flox counterparts (Fig. 7*A*), and IRE1α ablation led to dramatic decreases in the upregulation of *Nos2* mRNA as well as iNos protein expression in isolated KCs following I/R injury (Fig. 7, *B* and *C*). Furthermore, chronic LPS treatment could prominently and dose-dependently stimulate the iNos protein as well as *Nos2* mRNA expression, and loss of IRE1α markedly blunted it (Fig. 7, *D–G*). This is in line with our previous observation that IRE1α is crucial for LPS-induced iNos expression in bone-marrow-derived macrophages (42). In addition, inhibition by 4μ8C of IRE1α's RNase activity also decreased LPS-stimulated iNos protein expression in primary KCs (Fig. 7*H*). These results indicate that IRE1α RNase-dependent regulation of iNos may also contribute to hepatic I/R injury. It is very likely that IRE1α could promote the expression of iNos through its UPR effector XBP1s, which has been documented to drive its transcription in cultured HepG2 cell line under experimental ER stress (58) or in mouse astrocytes during chemical-induced neuroinflammation (59).

### Pharmacological inhibition of IRE1α RNase activity protects mice against hepatic I/R injury

Given that IRE1α acts through its RNase activity to promote NLRP3 inflammasome activation and iNos expression in KCs, we tested the pharmacologic effects of 4μ8C upon I/R-induced liver inflammation and injury in mice. To this end, administration of 4μ8C in I/R injured animals significantly reduced hepatic necrotic area, lowered their serum levels of ALT and AST, and decreased cell death in livers when compared with the vehicle control group (Fig. 8, *A–C*). Moreover, 4μ8C-treated animals exhibited significant reductions in liver infiltration of Ly6G^{+} neutrophils and in serum levels of proinflammatory cytokines/chemokines, including IL-1β, TNFα, CCL2, and CXCL10 (Fig. 9, *A* and *B*). Similar to the observations in MΦKO livers, 4μ8C inhibition of IRE1α RNase in I/R-injured mice resulted in decreased *Xbp1s* and *Erdj4* mRNA levels without affecting the expression of other UPR target genes (*Bip, Chop, Atf4*) in isolated KCs, in parallel with lower *Nos2* and *Ccl2*, but not *Il1b*, mRNA levels (Fig. 9, *C* and *D*). Notably, 4μ8C inhibited the IRE1α-XBP1s pathway, but did not significantly suppress the expression of inflammatory cytokines examined in isolated hepatocytes (Fig. S2). Consistently, immunoblot analyses showed that 4μ8C treatment reduced XBP1s protein production without altering eIF2α phosphorylation and led to significant decreases in NLRP3, c-Casp1, and iNos protein levels (Fig. 9*E*). Supporting the functional significance of 4μ8C suppression of iNos expression, administration of 1400W, a chemical iNos enzyme inhibitor (60), largely phenocopied the alleviating effects of the IRE1α inhibitor upon I/R-induced liver dysfunction and inflammation in mice (Fig. S3). Collectively, these results indicate that pharmacologically blocking the RNase activity of
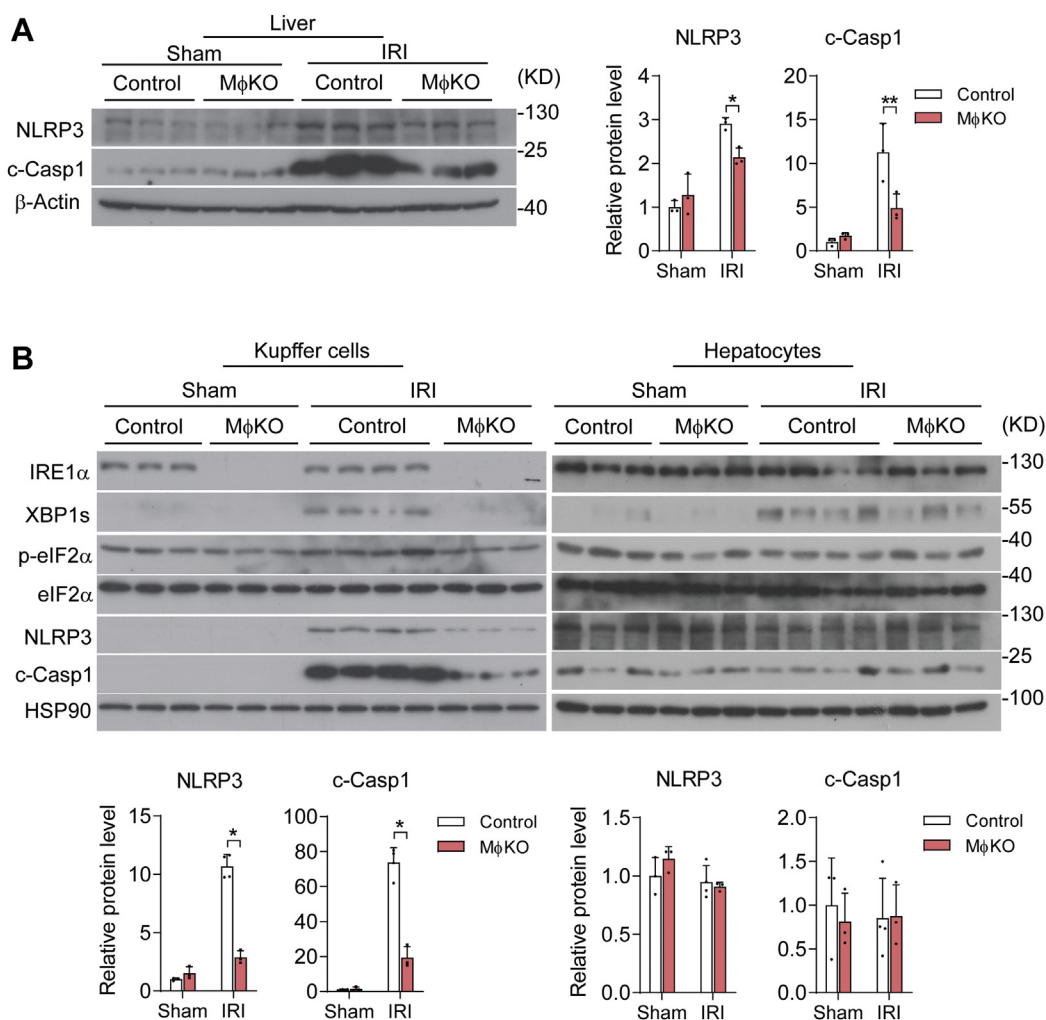
**Figure 5. IRE1α abrogation blunts the activation of NLRP3 inflammasome in Kupffer cells following I/R injury.** Control or MΦKO mice were subjected to sham or hepatic warm ischemia/reperfusion (n=3–4 per group). *A,* immunoblot analysis of NLRP3 and cleaved-Caspase1 (c-Casp1) in whole liver lysates. β-Actin was used as the loading control. Shown also is quantification of the relative protein levels of NLRP3 and c-Casp1. *B,* immunoblot analysis of the indicated proteins in lysates of freshly isolated Kupffer cells and hepatocytes. HSP90 was used as the loading control. The relative protein levels of NLRP3 and c-Casp1 were quantified. All data represent the mean ± SD after normalization to the mean value of the sham control group. *$p < 0.05$ and **$p < 0.01$ by two-way ANOVA. NLRP3, nucleotide-binding domain, leucine-rich repeat containing protein 3.

IRE1α can limit Kupffer-cell-mediated liver inflammation and damage during hepatic I/R injury.

## Discussion

As a common clinical issue resulting from various surgical procedures such as liver transplantation and hepatic resection, hepatic I/R injury can cause graft dysfunction and liver failure (12) and currently lacks effective therapeutic approaches. Validated pharmacologic targets are urgently needed for the development of novel clinical strategy to improve the outcomes of liver surgeries. Liver inflammation is a key feature of hepatic I/R injury, and multiple types of immune cells are involved in mediating the inflammatory damage in response to I/R-induced stress. In this study, we demonstrated a critical role for IRE1α in exacerbating hepatic I/R injury through promoting Kupffer-cell-mediated liver inflammatory responses. Importantly, we found that pharmacologic inhibition of IRE1α RNase activity could efficiently dampen liver

inflammation and alleviate hepatic I/R injury in mice. Our findings suggest that IRE1α in KCs represents a promising target for developing therapeutics for the prevention and treatment of IR-associated liver dysfunction.

Numerous studies have established that IRE1α serves as a multifunctional signal transducer in managing cellular stress responses and regulating diverse biological processes including cell fate decision, proliferation, metabolism, and immunity (22, 24–26, 29, 30). Upon activation, IRE1α exerts its regulatory actions mainly through its RNase activity-directed XBP1s production or RIDD control of select mRNA/microRNA stability (24–26, 29, 30). In accordance with its role in governing myeloid cell activation during inflammatory responses (41–43), our results revealed that IRE1α can augment the activation of KCs, presumably in response to hepatic danger-associated molecular pattern (DAMP) molecules generated under I/R-induced stress conditions (61). Mechanistically, IRE1α employs its RNase activity to promote NLRP3 inflammasome activation for IL-1β
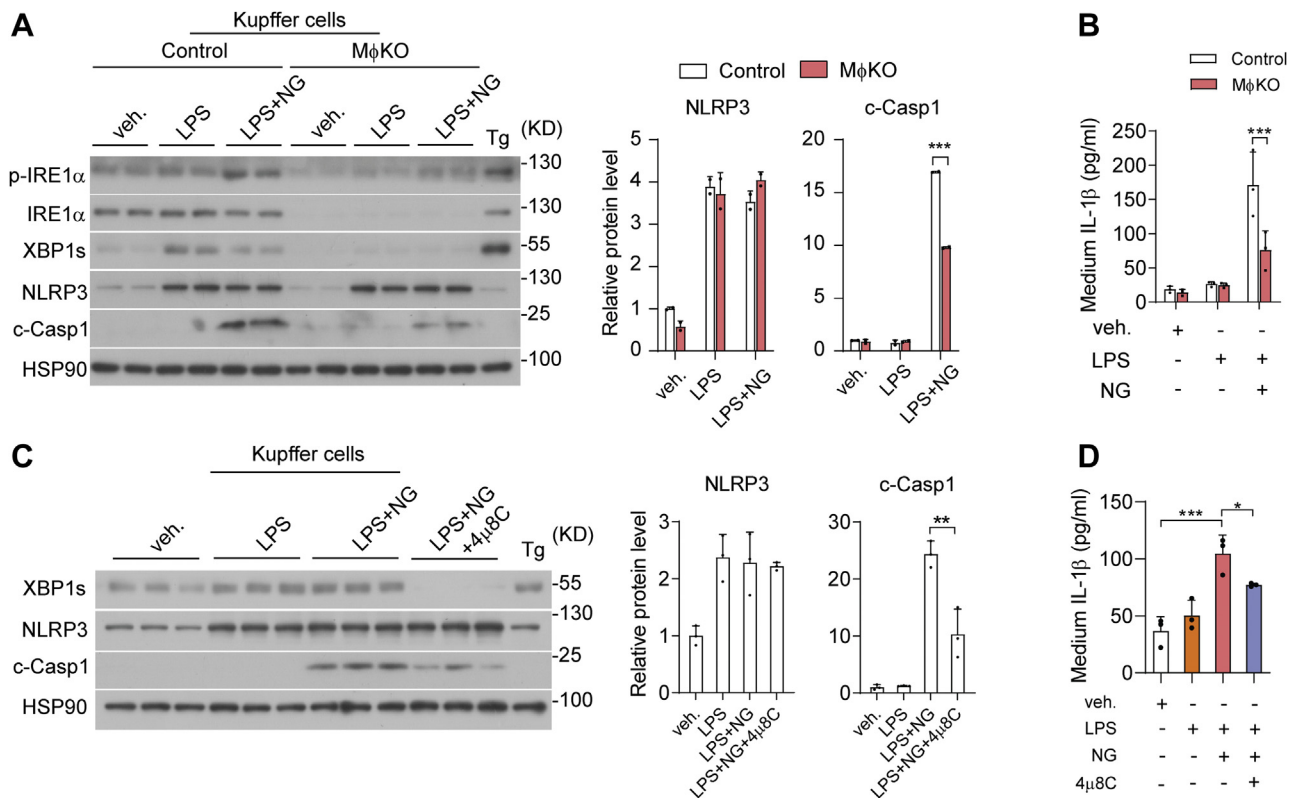
**Figure 6. IRE1α's RNase activity contributes to NLRP3 inflammasome activation and IL-1β production in Kupffer cells.** *A* and *B*, Kupffer cells freshly isolated from livers of male control or MΦKO mice were treated with PBS (veh.), or LPS (100 ng/ml) for 12 h or treated with LPS for 12 h plus Nigericin (NG; 20 μM) treatment for 30 min before harvest. Cells treated with thapsigargin (Tg, 1 μM) for 2 h were included as the ER stress control. *A*, immunoblot analysis of the indicated proteins in cell lysates. HSP90 was used as the loading control. The relative levels of NLRP3 and c-Casp1 proteins were quantified. *B*, ELISA analysis of IL-1β protein in the culture medium of control and MΦKO Kupffer cells. *C* and *D*, Kupffer cells from C57BL6 mice were likewise treated with DMSO (veh.), LPS (100 ng/ml), or LPS plus NG (20 μM) in the absence or presence of 4μ8C (10 μM). *C*, immunoblot analysis of the indicated proteins. The relative levels of NLRP3 and c-Casp1 proteins were quantified. *D*, ELISA analysis of IL-1β protein in the culture medium. All data represent the mean ± SD. *$p < 0.05$, **$p < 0.01$, and ***$p < 0.001$ by two-way ANOVA. NLRP3, nucleotide-binding domain, leucine-rich repeat containing protein 3.

production along with upregulation of iNos expression, which can collectively amplify liver inflammation to cause liver injury (6, 12, 61). Moreover, we found that IRE1α deficiency appeared to cause decreased protein level of NLRP3 in isolated primary KCs following I/R injury, but had no impact upon NLRP3 protein in LPS/NG-stimulated KCs. While this conceivably reflects the effects *in vivo* of other factors/cell types from the disrupted liver microenvironment inflicted by the I/R stress, it is likely that IRE1α in KCs mainly acts to promote the assembly of NLRP3 inflammasome in a manner that depends on its RNase activity. This is in line with reported findings that IRE1α is linked to inflammasome activation through thioredoxin-interacting protein (TXNIP), a promoting molecule in oxidative-stress-associated inflammasome activation (62), in other cell types, or upon stimulation by other stress stimuli (46, 63, 64). In addition, reported studies have also shown that XBP1 is implicated in the regulation by myeloid heat shock transcription factor 1 (HSF1)-β-catenin signaling of NLRP3 inflammasome activation during I/R injury in the liver (46), and β-catenin can interact with XBP1s in the context of hypoxia response (65). Given the complex mechanisms governing inflammasome assembly/activation in relation to mitochondrial damage and intracellular lipid flux during ischemic stress, it remains to be

further dissected whether TXNIP or XBP1s is directly involved in IRE1α-mediated inflammasome activation in KCs during I/R injury. In addition, the NLRP3 inflammasome is a critical sensor and mediator of the inflammatory response, which can be activated by a variety of external stimuli and regulated by many interrelated cellular pathways (62). Other, probably IRE1α-independent, signaling pathways may also be involved in activation of the NLRP3 inflammasome, *e.g.*, the NF-kB signaling (62) or PERK (46, 63, 64) pathways during ischemic stress. Interestingly, in an NLRP3 knockout mouse model, NLRP3 was shown to regulate chemokine-mediated functions and recruitment of neutrophils, thereby contributing to hepatic I/R injury independently of inflammasomes (6, 13). Therefore, it warrants further investigation whether IRE1α is also implicated in other NLRP3-related process.

It is worth noting that IRE1α also acts through its RNase activity to augment the expression of iNos in KCs, most likely in a similar fashion depending upon its downstream effector XBP1s as documented in other cell types (58, 59). Despite the controversial findings with regard to the role of iNos in hepatic I/R injury from genetic deletion studies (18–20), we found that pharmacologic blocking of iNos activity in mice with a selective iNos inhibitor 1400W could efficiently improve liver I/R injury. Importantly, the beneficial effects of 4μ8C inhibition of
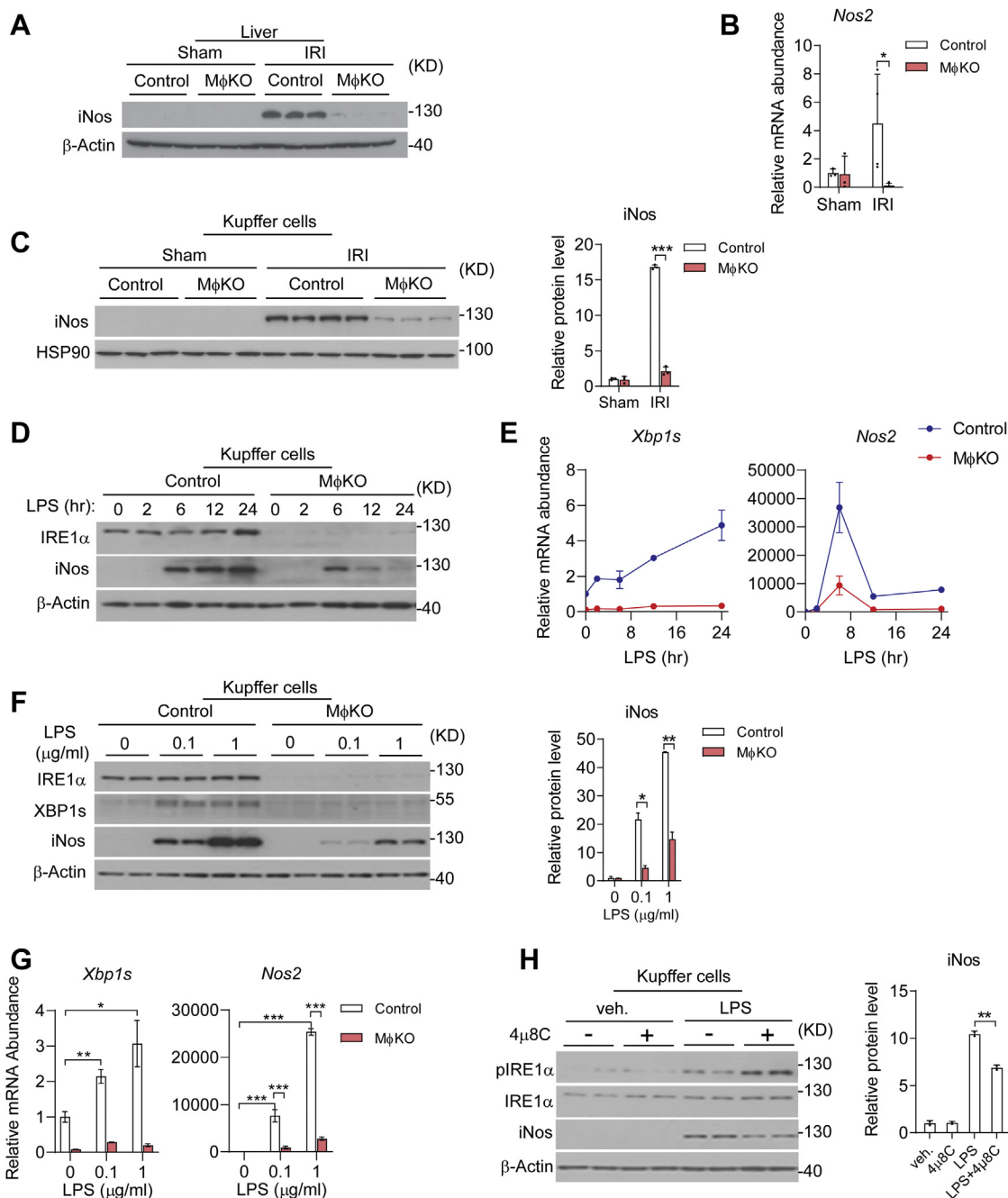
**Figure 7. IRE1α deficiency diminishes iNos expression in Kupffer cells.** *A–C,* control or MΦKO mice were subjected to sham or hepatic warm ischemia/reperfusion (n=3–4 per group). *A,* immunoblot analysis of iNos protein in liver lysates. β-Actin was used as the loading control. *B,* qRT-PCR analysis of the mRNA abundance of *Nos2* in isolated Kupffer cells. *C,* immunoblot analysis of iNos protein in freshly isolated Kupffer cells. HSP90 was used as the loading control. The relative levels of iNos protein were quantified. *D–G,* Kupffer cells were isolated from control and MΦKO mice. Cells were then treated with 100 ng/ml LPS for the indicated time intervals (*D* and *E*), or with 0.1 or 1 μg/ml LPS for 12 h (*F* and *G*). *D* and *F,* immunoblot analysis of IRE1α and iNos protein. *E* and *G,* qRT-PCR analysis of the mRNA abundance of *Xbp1s* and *Nos2. H,* primary Kupffer cells were treated with PBS (veh) or 100 ng/ml LPS with or without 10 μM 4μ8C. Immunoblot analysis of the indicated proteins. The relative levels of iNos protein were quantified. All data represent the mean ± SD. *p < 0.05, **p < 0.01, and ***p < 0.001 by one way or two-way ANOVA.

IRE1α RNase in mice upon hepatic I/R injury are accompanied by significant suppression of NLRP3 inflammasome activation as well as iNos expression in KCs. Therefore, there results support that multiple players, including both inflammasome activation and iNos upregulation, contribute to mediating IRE1α′s promoting effects upon liver I/R injury. Given that liver I/R is a dynamic process involving many cell types in eliciting sterile inflammation and hepatocyte damage (1, 2, 6, 66), we cannot exclude the potential, either direct or indirect, impacts of IRE1α deletion or its RNase inhibition upon recruitment and activation of other immune cells such as infiltrated monocytes/macrophages as exemplified by reported studies (26, 42, 43, 46, 67). Moreover, we have previously shown that in hepatocytes, IRE1α not only regulates nutrient

**Figure 8. Pharmacological inhibition of IRE1α RNase alleviates hepatic I/R injury.** Male C57BL6 mice were intraperitoneally injected daily with DMSO (veh) or 4μ8C (10 mg/kg body weight) for 3 days prior to hepatic I/R injury (n = 3 mice per group). *A*, representative images of hematoxylin and eosin staining of liver sections with the necrotic regions indicated. The area of necrosis per field was quantified. Scale bar, 100 μm. *B*, serum ALT and AST levels. *C*, representative images of TUNEL staining of liver sections. TUNEL-positive cells per field were quantified. Scale bar, 15 μm. All data represent the mean ± SD. *$p < 0.05$ and ***$p < 0.001$ by one-way ANOVA.

stress responses but also drives reparative regeneration and obesity-associated liver inflammation (68–71). Thus, it has yet to be further investigated if hepatocyte IRE1α also contributes to sterile inflammation and hepatocyte damage during hepatic I/R injury.

In conclusion, our current study has revealed that KC IRE1α responds to ischemic stress and promotes liver inflammatory injury caused by I/R. Targeted inhibition of the IRE1α pathway in myeloid cells offers a valuable translational opportunity for developing therapeutics against not only hepatic I/R injury-related conditions, but also other types of inflammatory liver diseases (72).

## Experimental procedures

### Animals

Wild-type C57/BL6 mice were purchased from the Experimental Animal Research Center of Hubei Province. Myeloid-specific IRE1α knockout mice (MΦKO) were generated by intercrossing floxed *Ern1* mice with the *lyz2*-Cre line as previously described (42). Mice were maintained in individual temperature-controlled ventilated cages with a 12-h light/dark cycle (7:00 AM light on) in a specific-pathogen-free (SPF) facility. All animal experiments were approved by the Animal Care and Use Committee of College of Life Sciences, Wuhan University.

### Hepatic ischemia/reperfusion injury mouse model

Mice were subjected to a 70% liver warm I/R surgery as described in detail (73). Briefly, upon anesthetization with sodium pentobarbital, male mice at ∼8–14 weeks of age were subjected to midline laparotomy to expose the liver. The middle and left portal vein branches were blocked for 60 min using atraumatic clamps to induce partial hepatic ischemia, and then the clamps were removed to allow for 6 h of reperfusion before mice were sacrificed. As a sham control, mice were subjected to the same surgical process except vasculature occlusion.

### Treatment of hepatic I/R injury with chemical inhibitors

For IRE1α RNase inhibition, mice were intraperitoneally (i.p.) injected daily with 4μ8C (10 mg per kg body weight; Targetmol, #T6363) or 10% DMSO, 40% PEG300, 5% Tween 80 in saline as vehicle control for 3 days before hepatic I/R surgery was performed. For iNOS inhibition, mice were injected with 1400W (35 mg per kg body weight; Targetmol, #T3491) or 10% DMSO, 40% PEG300, 5% Tween 80 in saline as vehicle control at 1 h prior to hepatic I/R surgery.

### Clodronate depletion of liver-resident macrophages

For depletion of liver-resident macrophages including KCs, animals were injected through tail vein with clodronate liposomes or control liposomes (200 μl per mouse, LIPOSOMA, #CP005005) at 24 h prior to hepatic I/R surgery.

### Histology, TUNEL analysis, and immunohistochemistry

Sections of liver tissues were fixed in 10% formalin for paraffin embedding. Paraffin-embedded liver sections were subjected to hematoxylin and eosin staining.

**Figure 9. Blocking IRE1α RNase attenuates Kupffer-cell-mediated inflammation during hepatic I/R injury.** *A,* immunohistochemical staining of Ly6G+ neutrophils in liver sections of the indicated group. Quantification of Ly6G+ cells is shown per field. Scale bar, 100 μm. *B,* ELISA analysis of serum levels of the indicated inflammatory cytokines. *C* and *D,* qRT-PCR analysis of the mRNA abundance of the indicated UPR (*C*) or inflammatory genes (*D*) in freshly isolated Kupffer cells. *E,* immunoblot analysis of the indicated proteins in lysates of freshly isolated Kupffer cells. HSP90 was used as the loading control. The relative levels of NLRP3, c-Casp1 and iNos proteins were quantified. All data represent the mean ± SD. *$p < 0.05$ and **$p < 0.01$ by one-way ANOVA. NLRP3, nucleotide-binding domain, leucine-rich repeat containing protein 3; UPR, unfolded protein response.

For immunohistochemical analysis, liver tissue sections were permeabilized with blocking buffer (3% bovine serum albumin) for 1 h after antigen retrieval and 3% $H_2O_2$ incubation. Then, the liver sections were incubated in Ly6G

antibodies (1:1000 dilution; Servicebio, #GB11229) overnight at 4 °C. After washing with PBS, samples were incubated with HRP-conjugated secondary antibody (1:1000 dilution; Servicebio, #GB23303) 1 h at 37 °C prior to the incubation with

Diaminobenzidine Tetrahydrochloride (DAB). Section images of H&E and IHC staining were visualized by a light microscope. Cell death was analyzed using the Dead End Fluorometric Tunel System (Promega, #G3250) according to the manufacturer's instructions. Signals of dead cells were visualized by fluorescence microscopy. Necrotic area, Ly6G+ neutrophils, and Tunel+ cells were quantified using Image J software.

### Serum measurements

Serum levels of TNFα (ABclonal, #RK00027), IL-1β (ABclonal, #RK00006), CCL-2 (ABclonal, #RK00381), and CXCL-10 (ABclonal, #RK00054) were measured using ELISA kits following manufacturers' instructions. Serum ALT and AST levels were measured using the Mindray kit (Mindray) according to the manufacturer's instructions.

### Isolation of hepatocytes and Kupffer cells

Hepatocytes and KCs were freshly isolated from mice as described (74). Briefly, livers were perfused *in situ* with HBSS solution and then with collagenase buffer (Collagenase type IV, Sigma, #C5138). Perfused livers were subsequently dissected and collected through a 70-μm nylon mesh cell strainer. Hepatocytes were separated from nonparenchymal cells (NPCs) by centrifugation three times at 50$g$ for 2 min. For isolation of KCs, NPCs were harvested by centrifugation at 1350$g$ for 5 min and resuspended in HBSS. Cells were then layered onto a 25%/50% two-step Percoll gradient (Sigma, #P4937) in a 50-ml centrifuge tube before centrifugation at 1800$g$ for 15 min at 4 °C. KCs enriched in the middle layer were collected for further analysis or allowed to attach onto culture plates in DMEM supplemented with 10% FBS, 10 mM HEPES, 2 mM GlutaMax, 100 U/ml penicillin, and 100 μg/ml streptomycin. For *in vitro* activation and inhibition assays, KCs were cultured overnight before treatment with 4μ8C (10 μM, Targetmol, #T6363), lipopolysaccharide (LPS, 100 ng/ml, Sigma, #L2630), and nigericin (NG, 20 μM, MCE, #HY-100381).

### Antibodies and immunoblot analysis

Lysates of cells or liver tissues were prepared with RIPA buffer (150 mM NaCl, 1% NP-40, 0.5% sodium deoxycholate, 0.1% SDS, and 50 mM Tris-HCl, pH 7.4) containing complete protease-inhibitor cocktail (Sigma). Proteins separated by SDS-PAGE were transferred onto a polyvinylidene difluoride (PVDF) membrane filter (Millipore). After incubation with the desired antibodies, blots were developed with Super-Signal West Pico Chemiluminescent substrate (Thermo Scientific) or Immobilon Western Chemiluminescent HRP substrate (Millipore). Antibodies used include: phosphorylated IRE1α (p-IRE1α, 1:1000 dilution; CUSABIO, #CSB-RA007795A724phHU), IRE1α (1:1000 dilution; CST, #3294), XBP1s (1:1000 dilution; abcam, #ab220783), phosphorylated eIF2α (1:1000 dilution; p-eIF2α, CST, #3398), eIF2α (1:1000 dilution; CST, #5324), iNos (1:1000 dilution; CST, #13120), NLRP3 (1:1000 dilution; CST, #15101), cleaved-Caspase1 (c-Casp1, 1:1000 dilution; abcam, #ab179515), HSP90 (1:1000 dilution; CST, #4877), and β-Actin (1:1000 dilution; ABclonal, #ac026).

### Quantitative RT–PCR

Total RNA was isolated from cells or liver tissues using TRIzol reagent (sigma). cDNA was synthesized with M-MLV reverse transcriptase and random hexamer primers (Invitrogen). Quantitative real-time PCR was performed with SYBR Green PCR reagents (Applied Biosystems) on an ABI 7500 system (Applied Biosystems). *β-Actin* was used as an internal control for normalization. Primers sequences used are as follows:

*β-Actin* Forward: 5′-AGTGTGACGTTGACATCCGTA-3′;
*β-Actin* Reverse: 5′-GCCAGAGCAGTAATCTCCTTCT-3′;
*Xbp1s* Forward: 5′-CTGAGTCCGAATCAGGTGCAG-3;
*Xbp1s* Reverse: 5′-GTCCATGGGAAGATGTTCTGG-3;
*Erdj4* Forward: 5′-ATAAAAGCCCTGATGCTGAAGC-3;
*Erdj4* Reverse: 5′-GCCATTGGTAAAAGCACTGTGT-3;
*Bip* Forward: 5′-ACTTGGGGACCACCTATTCCT-3;
*Bip* Reverse: 5′-ATCGCCAATCAGACGCTCC-3;
*Chop* Forward: 5′-CTGGAAGCCTGGTATGAGGAT-3;
*Chop* Reverse: 5′-CAGGGTCAAGAGTAGTGAAGGT-3;
*Atf4* Forward: 5′-CCTTCGACCAGTCGGGTTTG-3;
*Atf4* Reverse: 5′-CTGTCCCGGAAAAGGCATCC-3;
*Nos2* Forward: 5′-ACATCGACCCGTCCACAGTAT-3;
*Nos2* Reverse: 5′-CAGAGGGGTAGGCTTGTCTC-3;
*Tnfa* Forward: 5′-GACGTGGAACTGGCAGAAGAG-3;
*Tnfa* Reverse: 5′-ACCGCCTGGAGTTCTGGAA-3;
*Il1b* Forward: 5′-GCAACTGTTCCTGAACTCAACT-3;
*Il1b* Reverse: 5′-ATCTTTTGGGGTCCGTCAACT-3;
*Ccl2* Forward: 5′-TTAAAAACCTGGATCGGAACCAA-3;
*Ccl2* Reverse: 5′-GCATTAGCTTCAGATTTACGGGT-3.

### Statistical analysis

All data are presented as the mean ± SD. Statistical analysis was performed with unpaired two-tailed Student's $t$ test or one-way or two-way analysis of variance (ANOVA) followed by Bonferroni's test using GraphPad Prism 8.0. $p < 0.05$ was considered to be statistically significant.

### Data availability

The data that support the findings of this study are available from the corresponding author upon reasonable request.

*Abbreviations*—The abbreviations used are: ALT, alanine aminotransferase; AST, aspartate aminotransferase; ATF6, activating transcription factor 6; ER, endoplasmic reticulum; iNos, inducible nitric oxide synthase; I/R, ischemia/reperfusion; IRE1, inositol-requiring enzyme 1; KC, Kupffer cell; NLRP3, nucleotide-binding domain, leucine-rich repeat containing protein 3; PERK, protein kinase RNA-like endoplasmic reticulum kinase; RIDD, regulated IRE1-dependent decay; ROS, reactive oxygen species; TXNIP, thioredoxin-interacting protein; UPR, unfolded protein response; XBP1, X-box binding protein 1.

## References

1. Zhai, Y., Petrowsky, H., Hong, J. C., Busuttil, R. W., and Kupiec-Weglinski, J. W. (2013) Ischaemia-reperfusion injury in liver transplantation–From bench to bedside. *Nat. Rev. Gastroenterol. Hepatol.* **10**, 79–89
2. Rakic, M., Patrlj, L., Amic, F., Aralica, G., and Grgurevic, I. (2018) Comparison of hepatoprotective effect from ischemia-reperfusion injury of remote ischemic preconditioning of the liver vs local ischemic preconditioning of the liver during human liver resections. *Int. J. Surg.* **54**, 248–253
3. Zhang, X. J., Cheng, X., Yan, Z. Z., Fang, J., Wang, X., Wang, W., Liu, Z. Y., Shen, L. J., Zhang, P., Wang, P. X., Liao, R., Ji, Y. X., Wang, J. Y., Tian, S., Zhu, X. Y., *et al.* (2018) An ALOX12-12-HETE-GPR31 signaling axis is a key mediator of hepatic ischemia-reperfusion injury. *Nat. Med.* **24**, 73–83
4. Quesnelle, K. M., Bystrom, P. V., and Toledo-Pereyra, L. H. (2015) Molecular responses to ischemia and reperfusion in the liver. *Arch. Toxicol.* **89**, 651–657
5. Yang, Q., Liu, Y., Shi, Y., Zheng, M., He, J., and Chen, Z. (2013) The role of intracellular high-mobility group box 1 in the early activation of Kupffer cells and the development of Con A-induced acute liver failure. *Immunobiology* **218**, 1284–1292
6. Huang, H., Chen, H. W., Evankovich, J., Yan, W., Rosborough, B. R., Nace, G. W., Ding, Q., Loughran, P., Beer-Stolz, D., Billiar, T. R., Esmon, C. T., and Tsung, A. (2013) Histones activate the NLRP3 inflammasome in Kupffer cells during sterile inflammatory liver injury. *J. Immunol.* **191**, 2665–2679
7. Zhai, Y., Busuttil, R. W., and Kupiec-Weglinski, J. W. (2011) Liver ischemia and reperfusion injury: New insights into mechanisms of innate-adaptive immune-mediated tissue inflammation. *Am. J. Transpl.* **11**, 1563–1569
8. Nakamura, K., Zhang, M., Kageyama, S., Ke, B., Fujii, T., Sosa, R. A., Reed, E. F., Datta, N., Zarrinpar, A., Busuttil, R. W., Araujo, J. A., and Kupiec-Weglinski, J. W. (2017) Macrophage heme oxygenase-1-SIRT1-p53 axis regulates sterile inflammation in liver ischemia-reperfusion injury. *J. Hepatol.* **67**, 1232–1242
9. Ahmed, O., Robinson, M. W., and O'Farrelly, C. (2021) Inflammatory processes in the liver: Divergent roles in homeostasis and pathology. *Cell. Mol. Immunol.* **18**, 1375–1386
10. Dixon, L. J., Barnes, M., Tang, H., Pritchard, M. T., and Nagy, L. E. (2013) Kupffer cells in the liver. *Compr. Physiol.* **3**, 785–797
11. Krenkel, O., and Tacke, F. (2017) Liver macrophages in tissue homeostasis and disease. *Nat. Rev. Immunol.* **17**, 306–321
12. Jimenez-Castro, M. B., Cornide-Petronio, M. E., Gracia-Sancho, J., and Peralta, C. (2019) Inflammasome-mediated inflammation in liver ischemia-reperfusion injury. *Cells* **8**, 1131
13. Inoue, Y., Shirasuna, K., Kimura, H., Usui, F., Kawashima, A., Karasawa, T., Tago, K., Dezaki, K., Nishimura, S., Sagara, J., Noda, T., Iwakura, Y., Tsutsui, H., Taniguchi, S., Yanagisawa, K., *et al.* (2014) NLRP3 regulates neutrophil functions and contributes to hepatic ischemia-reperfusion injury independently of inflammasomes. *J. Immunol.* **192**, 4342–4351
14. Bogdan, C. (2001) Nitric oxide and the immune response. *Nat. Immunol.* **2**, 907–916
15. Nathan, C. (1997) Inducible nitric oxide synthase: What difference does it make? *J. Clin. Invest.* **100**, 2417–2423
16. MacMicking, J., Xie, Q. W., and Nathan, C. (1997) Nitric oxide and macrophage function. *Annu. Rev. Immunol.* **15**, 323–350
17. Koerber, K., Sass, G., Kiemer, A. K., Vollmar, A. M., and Tiegs, G. (2002) *In vivo* regulation of inducible no synthase in immune-mediated liver injury in mice. *Hepatology* **36**, 1061–1069
18. Hines, I. N., Harada, H., Bharwani, S., Pavlick, K. P., Hoffman, J. M., and Grisham, M. B. (2001) Enhanced post-ischemic liver injury in iNOS-deficient mice: A cautionary note. *Biochem. Biophys. Res. Commun.* **284**, 972–976
19. Hamada, T., Duarte, S., Tsuchihashi, S., Busuttil, R. W., and Coito, A. J. (2009) Inducible nitric oxide synthase deficiency impairs matrix metalloproteinase-9 activity and disrupts leukocyte migration in hepatic ischemia/reperfusion injury. *Am. J. Pathol.* **174**, 2265–2277
20. Kawachi, S., Hines, I. N., Laroux, F. S., Hoffman, J., Bharwani, S., Gray, L., Leffer, D., and Grisham, M. B. (2000) Nitric oxide synthase and post-ischemic liver injury. *Biochem. Biophys. Res. Commun.* **276**, 851–854
21. Walter, P., and Ron, D. (2011) The unfolded protein response: From stress pathway to homeostatic regulation. *Science* **334**, 1081–1086
22. Hetz, C., Zhang, K., and Kaufman, R. J. (2020) Mechanisms, regulation and functions of the unfolded protein response. *Nat. Rev. Mol. Cell Biol.* **21**, 421–438
23. Schroder, M., and Kaufman, R. J. (2005) The mammalian unfolded protein response. *Annu. Rev. Biochem.* **74**, 739–789
24. Cox, J. S., Shamu, C. E., and Walter, P. (1993) Transcriptional induction of genes encoding endoplasmic reticulum resident proteins requires a transmembrane protein kinase. *Cell* **73**, 1197–1206
25. Hetz, C. (2012) The unfolded protein response: Controlling cell fate decisions under ER stress and beyond. *Nat. Rev. Mol. Cell Biol.* **13**, 89–102
26. Hetz, C., Martinon, F., Rodriguez, D., and Glimcher, L. H. (2011) The unfolded protein response: Integrating stress signals through the stress sensor IRE1alpha. *Physiol. Rev.* **91**, 1219–1243
27. Hollien, J., and Weissman, J. S. (2006) Decay of endoplasmic reticulum-localized mRNAs during the unfolded protein response. *Science* **313**, 104–107
28. Maurel, M., Chevet, E., Tavernier, J., and Gerlo, S. (2014) Getting RIDD of RNA: IRE1 in cell fate regulation. *Trends Biochem. Sci.* **39**, 245–254
29. Malhi, H., and Kaufman, R. J. (2011) Endoplasmic reticulum stress in liver disease. *J. Hepatol.* **54**, 795–809
30. Huang, S., Xing, Y., and Liu, Y. (2019) Emerging roles for the ER stress sensor IRE1alpha in metabolic regulation and disease. *J. Biol. Chem.* **294**, 18726–18741
31. Hotamisligil, G. S. (2010) Endoplasmic reticulum stress and the inflammatory basis of metabolic disease. *Cell* **140**, 900–917
32. Hetz, C., and Glimcher, L. H. (2011) Protein homeostasis networks in physiology and disease. *Curr. Opin. Cell Biol.* **23**, 123–125
33. Liu, X., and Green, R. M. (2019) Endoplasmic reticulum stress and liver diseases. *Liver Res.* **3**, 55–64
34. Emadali, A., Nguyen, D. T., Rochon, C., Tzimas, G. N., Metrakos, P. P., and Chevet, E. (2005) Distinct endoplasmic reticulum stress responses are triggered during human liver transplantation. *J. Pathol.* **207**, 111–118

35. Bailly-Maitre, B., Fondevila, C., Kaldas, F., Droin, N., Luciano, F., Ricci, J. E., Croxton, R., Krajewska, M., Zapata, J. M., Kupiec-Weglinski, J. W., Farmer, D., and Reed, J. C. (2006) Cytoprotective gene bi-1 is required for intrinsic protection from endoplasmic reticulum stress and ischemia-reperfusion injury. *Proc. Natl. Acad. Sci. U. S. A.* **103**, 2809–2814

36. Duvigneau, J. C., Kozlov, A. V., Zifko, C., Postl, A., Hartl, R. T., Miller, I., Gille, L., Staniek, K., Moldzio, R., Gregor, W., Haindl, S., Behling, T., Redl, H., and Bahrami, S. (2010) Reperfusion does not induce oxidative stress but sustained endoplasmic reticulum stress in livers of rats subjected to traumatic-hemorrhagic shock. *Shock* **33**, 289–298

37. Liu, J., Ren, F., Cheng, Q., Bai, L., Shen, X., Gao, F., Busuttil, R. W., Kupiec-Weglinski, J. W., and Zhai, Y. (2012) Endoplasmic reticulum stress modulates liver inflammatory immune response in the pathogenesis of liver ischemia and reperfusion injury. *Transplantation* **94**, 211–217

38. Yang, F., Wang, S., Liu, Y., Zhou, Y., Shang, L., Feng, M., Yuan, X., Zhu, W., and Shi, X. (2018) IRE1alpha aggravates ischemia reperfusion injury of fatty liver by regulating phenotypic transformation of kupffer cells. *Free Radic. Biol. Med.* **124**, 395–407

39. Liu, D., Liu, X., Zhou, T., Yao, W., Zhao, J., Zheng, Z., Jiang, W., Wang, F., Aikhionbare, F. O., Hill, D. L., Emmett, N., Guo, Z., Wang, D., Yao, X., and Chen, Y. (2016) IRE1-RACK1 axis orchestrates ER stress preconditioning-elicited cytoprotection from ischemia/reperfusion injury in liver. *J. Mol. Cell Biol.* **8**, 144–156

40. Garfinkel, B. P., and Hotamisligil, G. S. (2017) ER stress promotes inflammation through Re-wIREd macrophages in obesity. *Mol. Cell* **66**, 731–733

41. Martinon, F., Chen, X., Lee, A. H., and Glimcher, L. H. (2010) TLR activation of the transcription factor XBP1 regulates innate immune responses in macrophages. *Nat. Immunol.* **11**, 411–418

42. Shan, B., Wang, X., Wu, Y., Xu, C., Xia, Z., Dai, J., Shao, M., Zhao, F., He, S., Yang, L., Zhang, M., Nan, F., Li, J., Liu, J., Liu, J., *et al.* (2017) The metabolic ER stress sensor IRE1alpha suppresses alternative activation of macrophages and impairs energy expenditure in obesity. *Nat. Immunol.* **18**, 519–529

43. Qiu, Q., Zheng, Z., Chang, L., Zhao, Y. S., Tan, C., Dandekar, A., Zhang, Z., Lin, Z., Gui, M., Li, X., Zhang, T., Kong, Q., Li, H., Chen, S., Chen, A., *et al.* (2013) Toll-like receptor-mediated IRE1alpha activation as a therapeutic target for inflammatory arthritis. *EMBO J.* **32**, 2477–2490

44. Bronner, D. N., Abuaita, B. H., Chen, X., Fitzgerald, K. A., Nunez, G., He, Y., Yin, X. M., and O'Riordan, M. X. (2015) Endoplasmic reticulum stress activates the inflammasome via NLRP3- and caspase-2-driven mitochondrial damage. *Immunity* **43**, 451–462

45. Yue, S., Zhu, J., Zhang, M., Li, C., Zhou, X., Zhou, M., Ke, M., Busuttil, R. W., Ying, Q. L., Kupiec-Weglinski, J. W., Xia, Q., and Ke, B. (2016) The myeloid heat shock transcription factor 1/beta-catenin axis regulates NLR family, pyrin domain-containing 3 inflammasome activation in mouse liver ischemia/reperfusion injury. *Hepatology* **64**, 1683–1698

46. Talty, A., Deegan, S., Ljujic, M., Mnich, K., Naicker, S. D., Quandt, D., Zeng, Q., Patterson, J. B., Gorman, A. M., Griffin, M. D., Samali, A., and Logue, S. E. (2019) Inhibition of IRE1alpha RNase activity reduces NLRP3 inflammasome assembly and processing of pro-IL1beta. *Cell Death Dis.* **10**, 622

47. Li, C., Jin, Y., Wei, S., Sun, Y., Jiang, L., Zhu, Q., Farmer, D. G., Busuttil, R. W., Kupiec-Weglinski, J. W., and Ke, B. (2019) Hippo signaling controls NLR family pyrin domain containing 3 activation and governs immunoregulation of mesenchymal stem cells in mouse liver injury. *Hepatology* **70**, 1714–1731

48. Robblee, M. M., Kim, C. C., Porter Abate, J., Valdearcos, M., Sandlund, K. L., Shenoy, M. K., Volmer, R., Iwawaki, T., and Koliwad, S. K. (2016) Saturated fatty acids engage an IRE1alpha-dependent pathway to activate the NLRP3 inflammasome in myeloid cells. *Cell Rep.* **14**, 2611–2623

49. Zhu, P., Duan, L., Chen, J., Xiong, A., Xu, Q., Zhang, H., Zheng, F., Tan, Z., Gong, F., and Fang, M. (2011) Gene silencing of NALP3 protects against liver ischemia-reperfusion injury in mice. *Hum. Gene Ther.* **22**, 853–864

50. Martinon, F., Burns, K., and Tschopp, J. (2002) The inflammasome: A molecular platform triggering activation of inflammatory caspases and processing of proIL-beta. *Mol. Cell* **10**, 417–426

51. Agostini, L., Martinon, F., Burns, K., McDermott, M. F., Hawkins, P. N., and Tschopp, J. (2004) NALP3 forms an IL-1beta-processing inflammasome with increased activity in Muckle-Wells autoinflammatory disorder. *Immunity* **20**, 319–325

52. Swanson, K. V., Deng, M., and Ting, J. P. (2019) The NLRP3 inflammasome: Molecular activation and regulation to therapeutics. *Nat. Rev. Immunol.* **19**, 477–489

53. Sitia, G., Iannacone, M., Aiolfi, R., Isogawa, M., van Rooijen, N., Scozzesi, C., Bianchi, M. E., von Andrian, U. H., Chisari, F. V., and Guidotti, L. G. (2011) Kupffer cells hasten resolution of liver immunopathology in mouse models of viral hepatitis. *PLoS Pathog.* **7**, e1002061

54. Jordan, M. B., van Rooijen, N., Izui, S., Kappler, J., and Marrack, P. (2003) Liposomal clodronate as a novel agent for treating autoimmune hemolytic anemia in a mouse model. *Blood* **101**, 594–601

55. Katsnelson, M. A., Rucker, L. G., Russo, H. M., and Dubyak, G. R. (2015) K+ efflux agonists induce NLRP3 inflammasome activation independently of Ca2+ signaling. *J. Immunol.* **194**, 3937–3952

56. Cross, B. C., Bond, P. J., Sadowski, P. G., Jha, B. K., Zak, J., Goodman, J. M., Silverman, R. H., Neubert, T. A., Baxendale, I. R., Ron, D., and Harding, H. P. (2012) The molecular basis for selective inhibition of unconventional mRNA splicing by an IRE1-binding small molecule. *Proc. Natl. Acad. Sci. U. S. A.* **109**, E869–878

57. Volkmann, K., Lucas, J. L., Vuga, D., Wang, X., Brumm, D., Stiles, C., Kriebel, D., Der-Sarkissian, A., Krishnan, K., Schweitzer, C., Liu, Z., Malyankar, U. M., Chiovitti, D., Canny, M., Durocher, D., *et al.* (2011) Potent and selective inhibitors of the inositol-requiring enzyme 1 endoribonuclease. *J. Biol. Chem.* **286**, 12743–12755

58. Guo, F., Lin, E. A., Liu, P., Lin, J., and Liu, C. (2010) XBP1U inhibits the XBP1S-mediated upregulation of the iNOS gene expression in mammalian ER stress response. *Cell Signal.* **22**, 1818–1828

59. Wheeler, M. A., Jaronen, M., Covacu, R., Zandee, S. E. J., Scalisi, G., Rothhammer, V., Tjon, E. C., Chao, C. C., Kenison, J. E., Blain, M., Rao, V. T. S., Hewson, P., Barroso, A., Gutierrez-Vazquez, C., Prat, A., *et al.* (2019) Environmental control of astrocyte pathogenic activities in CNS inflammation. *Cell* **176**, 581–596.e18

60. Garvey, E. P., Oplinger, J. A., Furfine, E. S., Kiff, R. J., Laszlo, F., Whittle, B. J., and Knowles, R. G. (1997) 1400W is a slow, tight binding, and highly selective inhibitor of inducible nitric-oxide synthase *in vitro* and *in vivo*. *J. Biol. Chem.* **272**, 4959–4963

61. Szabo, G., and Petrasek, J. (2015) Inflammasome activation and function in liver disease. *Nat. Rev. Gastroenterol. Hepatol.* **12**, 387–400

62. Zhou, R., Tardivel, A., Thorens, B., Choi, I., and Tschopp, J. (2010) Thioredoxin-interacting protein links oxidative stress to inflammasome activation. *Nat. Immunol.* **11**, 136–140

63. Lerner, A. G., Upton, J. P., Praveen, P. V., Ghosh, R., Nakagawa, Y., Igbaria, A., Shen, S., Nguyen, V., Backes, B. J., Heiman, M., Heintz, N., Greengard, P., Hui, S., Tang, Q., Trusina, A., *et al.* (2012) IRE1alpha induces thioredoxin-interacting protein to activate the NLRP3 inflammasome and promote programmed cell death under irremediable ER stress. *Cell Metab.* **16**, 250–264

64. Oslowski, C. M., Hara, T., O'Sullivan-Murphy, B., Kanekura, K., Lu, S., Hara, M., Ishigaki, S., Zhu, L. J., Hayashi, E., Hui, S. T., Greiner, D., Kaufman, R. J., Bortell, R., and Urano, F. (2012) Thioredoxin-interacting protein mediates ER stress-induced beta cell death through initiation of the inflammasome. *Cell Metab.* **16**, 265–273

65. Xia, Z., Wu, S., Wei, X., Liao, Y., Yi, P., Liu, Y., Liu, J., and Liu, J. (2019) Hypoxic ER stress suppresses beta-catenin expression and promotes cooperation between the transcription factors XBP1 and HIF1alpha for cell survival. *J. Biol. Chem.* **294**, 13811–13821

66. Eltzschig, H. K., and Eckle, T. (2011) Ischemia and reperfusion–From mechanism to translation. *Nat. Med.* **17**, 1391–1401

67. Tufanli, O., Telkoparan Akillilar, P., Acosta-Alvear, D., Kocaturk, B., Onat, U. I., Hamid, S. M., Cimen, I., Walter, P., Weber, C., and Erbay, E. (2017) Targeting IRE1 with small molecules counteracts progression of atherosclerosis. *Proc. Natl. Acad. Sci. U. S. A.* **114**, E1395–E1404

68. Mao, T., Shao, M., Qiu, Y., Huang, J., Zhang, Y., Song, B., Wang, Q., Jiang, L., Liu, Y., Han, J. D., Cao, P., Li, J., Gao, X., Rui, L., Qi, L., *et al.*

(2011) PKA phosphorylation couples hepatic inositol-requiring enzyme 1alpha to glucagon signaling in glucose metabolism. *Proc. Natl. Acad. Sci. U. S. A.* **108**, 15852–15857

69. Shao, M., Shan, B., Liu, Y., Deng, Y., Yan, C., Wu, Y., Mao, T., Qiu, Y., Zhou, Y., Jiang, S., Jia, W., Li, J., Li, J., Rui, L., Yang, L., *et al.* (2014) Hepatic IRE1alpha regulates fasting-induced metabolic adaptive programs through the XBP1s-PPARalpha axis signalling. *Nat. Commun.* **5**, 3528

70. Wu, Y., Shan, B., Dai, J., Xia, Z., Cai, J., Chen, T., Lv, S., Feng, Y., Zheng, L., Wang, Y., Liu, J., Fang, J., Xie, D., Rui, L., Liu, J., *et al.* (2018) Dual role for inositol-requiring enzyme 1alpha in promoting the development of hepatocellular carcinoma during diet-induced obesity in mice. *Hepatology* **68**, 533–546

71. Liu, Y., Shao, M., Wu, Y., Yan, C., Jiang, S., Liu, J., Dai, J., Yang, L., Li, J., Jia, W., Rui, L., and Liu, Y. (2015) Role for the endoplasmic reticulum stress sensor IRE1alpha in liver regenerative responses. *J. Hepatol.* **62**, 590–598

72. Tacke, F. (2017) Targeting hepatic macrophages to treat liver diseases. *J. Hepatol.* **66**, 1300–1312

73. Yan, Z. Z., Huang, Y. P., Wang, X., Wang, H. P., Ren, F., Tian, R. F., Cheng, X., Cai, J., Zhang, Y., Zhu, X. Y., She, Z. G., Zhang, X. J., Huang, Z., and Li, H. (2019) Integrated omics reveals tollip as an regulator and therapeutic target for hepatic ischemia-reperfusion injury in mice. *Hepatology* **70**, 1750–1769

74. Bourgognon, M., Klippstein, R., and Al-Jamal, K. T. (2015) Kupffer cell isolation for nanoparticle toxicity testing. *J. Vis. Exp.* **18**, e52989